Heliyon 6 (2020) e04938

Contents lists available at ScienceDirect

Heliyon

journal homepage: www.cell.com/heliyon

Research article

Micellar effects and analytical applications of nitro substitution in 4-Nitro-*N*-alkyl-1,8-naphthalimide by cysteine derivatives

V.S. Martins [a], E.R. Triboni [b], J.B.S. Bonilha [c,†], L.M. Gonçalves [a], L. Mortara [a], L.A.C. Carvalho [a], B.R. Manda [a], C.D. Lacerda [a], F.C. Meotti [a], M.J. Politi [a], H. Chaimovich [a], I.M. Cuccovia [a,*]

[a] Departamento de Bioquímica, Instituto de Química, Universidade de São Paulo, Brazil
[b] Escola de Engenharia de Lorena da Universidade de São Paulo, Departamento de Engenharia Química (DEQUI), Lorena, SP, Brazil
[c] Faculdade de Filosofia Ciências e Letras da Universidade de São Paulo, FFCLRP, Ribeirão Preto, SP, Brazil

ARTICLE INFO

Keywords:
Analytical chemistry
Organic chemistry
Thiol levels
Micellar solutions
Fluorescence assay
Protein thiols

ABSTRACT

The aromatic nucleophilic substitution reactions of the nitro group of 4-Nitro-*N*-alkyl-1,8-naphthalimides by thiolate anions produce fluorescent derivatives and their rates are strongly accelerated by micelles of hexadecyltrimethylammonium chloride even at low pH. Acceleration factors of this reactions can reach million-fold. As the products are oxidant-insensible, this reaction allows the determination of SH- containing compounds such as cysteine, glutathione or proteins even in oxidative conditions. Limits of detection are as low as 5×10^{-7} M, ten times lower than the limit for the classic 5,5′-dithiobis-(2-nitrobenzoic) acid method. Moreover, this reaction can be developed at pHs between 6.5 and 7.5 thereby diminishing the rate of spontaneous oxidation of the thiols. In addition, we demonstrated that 4-Nitro-*N*-alkyl-1,8-naphthalimides can be used to evidence SH groups in peptides, proteins and living cells.

1. Introduction

Organelles of living cells maintain different pHs, segregate ions, proteins, enzymes, and nucleic acids, maintaining dynamic equilibrium and allowing strictly controlled macromolecule and ion exchange through the compartments. Furthermore, the complexity of the enzymatic reactions is such that, in some cases, a single amino acid, such as Cysteine, Cys, can participate in various reaction types. Enzymes such as oxidases, reductases, cysteine proteases, peroxidases, transferases, kinases, phosphatases, and disulfide isomerases contain Cys at the active site, and catalyze different reactions in several cellular compartments [1]. Cys participates also in the maintenance of protein structure forming disulfide bridges, and is part of peptides, such as glutathione (γ-Glu–Cys–Gly, GSH), a vital component of the redox balance that reaches intracellular concentrations of 1 mM [2].

The pK_a of the thiol group of Cys is 8.56 or 10.03, depending on the protonation state of the amino group [3, 4]. The –SH group of Cys is, therefore, protonated at physiological pH's in lysosomes (pH = 4.5) or cytosol (pH = 7.4) [1,5]. The SH reactivity of most Cys in proteins or peptides is much lower than that of the thiolate (RS^-), the latter being a much better nucleophile [6, 7].

The pK_a of weak acids, such as R–SH is critically dependent on solvent and medium composition [8], and protein folding may determine local environments where the SH of Cys residue is located. In some proteins, the thiolate form of Cys is stabilized by lysine or arginine residues, even at low external pH. Charge–charge interactions, hydrogen bonds, desolvation, and helix–dipole effects are generally invoked to rationalize perturbed pK_as of –SH group of Cys residue [9, 10, 11].

An interesting reaction involving thiols is the substitution reaction of nitro-groups of 4-Nitro-1,8-naphthalic anhydrides (NNA), which forms a highly fluorescent thioether [12]. The reactions of NNA with thiols of amino acids and peptides such as Cys, GSH, and homocysteine, were studied at 50 °C, in dimethylformamide (DMF)/water mixtures (9:1). As the water percentage in the mixture increases, the reaction rate reaches a maximum, and above 30 % water, the rate decreases sharply. The high fluorescence of the products is a convenient property for thiol detection. A practical problem of this slow reaction is the need for organic solvent (DMF/Water), and high temperature (50 °C) for completion. Naphthalic anhydrides, with different substitutions at the 4-position of the

* Corresponding author.
E-mail address: imcuccov@iq.usp.br (I.M. Cuccovia).
† In memoriam.

https://doi.org/10.1016/j.heliyon.2020.e04938
Received 21 May 2020; Received in revised form 26 July 2020; Accepted 10 September 2020

naphthalene ring, such as 4-methylsulfonyl-*N*-*n*-butyl-1, 8-naphthalimide (MSBN), detect Cys and other thiols [13], but in ethanol/PBS 50:50 mixture, and the reaction time is at least one hour.

The substitution reaction of the nitro group (-NO_2) by thiols (Scheme 1) with 4-nitro-*N*-butyl-naphthalimide, 4-nitro-NBN, is particularly attractive because the reaction rate is medium dependent and the products are highly fluorescent, being also an excellent option as a probe for determination of low amounts of thiols. The second-order rate constant of the reaction of 4-nitro-NBN with n-heptanethiol, in basic methanol/(Water + MeOH) mixtures, (X_{MeOH}) [14], increases markedly with X_{MeOH} reaching a maximum of ca. four times the reaction rate in water at X_{MeOH} = 0.5 and decreases to the lowest value in pure methanol. Due to the high solvent sensibility of the reaction of nitro-naphthalimides with thiols, the kinetics of the nucleophilic substitution of the –NO_2 of 4-nitro-NBN by n-heptanethiol (C_7SH), thiophenol (PheSH) and 2-hydroxy-1-ethanethiol (2-HE-SH) were studied in micelles of hexadecyltrimethylammonium chloride, CTAC [15]. CTAC micelles increase the reaction rates of thiol-containing substrates with 4-Nitro-NBN by factors of 1×10^5 (for C_7SH) and 4×10^5 (PheSH) when compared with the rates in water. The reactions were analyzed using the ion-exchange model [16], and the second-order rate constant in the micellar phase, k_2^m, for all reaction were determined. The values of k_2^m are only two times higher than the rate constants in water, k_2^0, when the nucleophile was PheSH, and 20 times lower compared to C_7SH. Reagent concentration in the micellar phase and changes in the pK_a of the thiols account for the rate acceleration.

As the products of thiols with nitro-naphthalimides are highly fluorescent, it is convenient to use this reaction as an analytical tool to determine the concentration of thiols in biological compounds such as peptides and proteins. The standard method used for thiol quantification in proteins since 1959, the Ellman's method [17], uses 5,5′-dithio-bis-(2-nitrobenzoic acid), DTNB, which rapidly reacts with thiols, at pH 8.0, and the reaction product, 2,5-carboxy-nitro-thiobenzoic acid, TNB, is detected at 412 nm. However, TNB is sensitive to the presence of oxidants, leading to TNB re-oxidation [18]. Another probe for SH group determination is 4,4′-dithiopyridine (DTDP), which yields a product with high molar extinction coefficient (near 21,000 at 342 nm, at pHs between 4 and 7.4) but the detection wavelength of the product is low (324 nm) [19].

Herein we describe the aromatic nucleophilic substitution of –NO_2 of 4-nitro-NBN and 4-nitro-1,8-naphthalimide-N-ethylene-N, N′-dimethyl-N″-hexadecyl bromide (4-nitro-NEHN) by Cys, GSH and hexadecilcysteinamide, HCys (Scheme 1), in water and CTAC micelles and analyzed the micellar effects on the pK_as of the thiols and their reaction rates. These information's allowed the development of a new, sensitive, and oxidant stable method for determining the –SH contents of proteins using the enzyme peroxiredoxin 2, PRDX2, as a model. Moreover, we demonstrated that 4-nitro-NBN reacts with SH groups intracellularly.

2. Material and methods

Glutathione (GSH) and 5, 5′-dithio-bis-(2-nitrobenzoic acid), DTNB, from Sigma-Aldrich and cysteine chloride monohydrate (Cys), from Merck, were used without purification.

Buffers: 2-Amino-2-hydroxymethyl-propane-1,3-diol (Tris), (2-(N-morpholino)ethanesulfonic acid hydrate (MES), and 3-(cyclohexylamino)-2-hydroxy-1-propanesulfonic acid (CAPSO) were from Sigma-Aldrich. Tris(2-carboxyethyl)phosphine hydrochloride (TCEP), from Sigma-Aldrich, was used in the pK_a determination of thiols to avoid oxidation of the SH groups [22].

Thiol concentrations were determined with DTNB, using an ε = 14,150 at 412 nm [17, 23]. *N,N,N*-trimethyl-*N*-hexadecylammonium chloride, CTAC, (Aldrich) was recrystallized twice from methanol/acetone and its concentration in stock solutions was determined by Cl^- titration with $Hg(NO_3)_2$ using diphenylcarbazone, in acetone, as indicator [24].

2.1. Determination of the pK_{ap} of thiols in CTAC

The absorbance of the anionic form of HCys, $HCys^-$, was measured at 240 nm [3, 4] and that of GSH, GS^-, at 231 nm. All experiments were performed at 30 °C. The thiol pK_as, in the presence of detergent, were calculated using Eq. (1), where pK_{ap} is the apparent pK_a of the thiol in the presence of detergent. The pK_{ap}'s of thiols were determined measuring the absorbance of the anionic form of the thiol at only one pH, the experimental pH, pH_{exp}, at different CTAC concentrations, [CTAC]. The value of pH_{exp} was selected to obtain an adequate fraction of the thiol partially deprotonated in all detergent concentrations used.

$$pK_{ap} = pH_{exp} + log\frac{(Abs_A - Abs_\psi)}{(Abs_\psi - Abs_{HA})} \quad (1)$$

Abs_ψ, the absorbances of the anionic form of HCys and GSH at each detergent concentration, were measured in Tris/HCl 0.01 M buffer, pH 8.5 and pH 9.05 respectively. Abs_{HA}, the absorbance of the protonated form of the thiols, was measured in HCl 0.01 M, pH 2.0 and Abs_A, the absorbance of the dissociated form of the thiol, was measured in NaOH 0.001 M, pH 11. The values Abs_A and Abs_{HA} of HCys and GSH doesn't change with CTAC concentration, [CTAC]. The concentration of Cys, HCys and GSH were fixed at 5×10^{-5} M for pK_{ap} determinations. In these experiments, 1.04×10^{-4} M tris(2-carboxyethyl)phosphine (TCEP) was added to the cuvettes to avoid oxidation of the SH groups during absorbance determinations. Stock solutions of HCys (0.01M) in methanol and GSH (0.01 M) in water were maintained at 4 °C during the experiments.

2.2. Kinetics

The reactions of 4-nitro-NBN and 4-nitro-NEHN with thiols were followed at 400 nm in a Cary 3E spectrophotometer, in quartz cuvettes with 1.0 cm path length, using 2.5 mL total volume. All kinetics were performed at 30 °C. The buffers (0.01 M, except when indicated) used were: sodium acetate (pHs 5.0 and 5.5), MES (pHs 5.1; 5.3; 5.5; 6.0; 6.5 and 7.1), Tris/HCl (pH 7.0; 7.5), CAPSO, pH 10.6. Buffers were prepared with deionized water, saturated with N_2 before use to minimize thiol oxidation during the kinetics. No TCEP was used in the kinetic studies because it reacts with nitro-naphthalimides. Fluorescence measurements were performed in a Hitachi F-2000 spectrofluorimeter at 700 V.

2.3. General observation in all SH reactions

SH group concentrations, at the end of the reactions, were measured with DTNB. Under all the conditions, less than 2 % of SH were lost by oxidation at the end of the kinetics.

2.4. Kinetics of Cys and GSH with 4-nitro-NBN in water

The second-order rate constants of the reactions of 4-nitro-NBN with Cys and GSH in water, k_2^w, were determined in concentrated buffers (borate buffer, 0.15 M, pH 10.0 and CAPSO 0.15 M, pH 10.6). The stock solutions of Cys and GSH, in water, were 0.1 M and the concentration of the thiols was varied from 0.004 to 0.012 M to obtain the second-order rate constants in water. The final pH of reaction mixture decreased by less than 0.6 pH units (borate buffer, initial pHs 10.0 to 9.46 and, CAPSO, from pH10.60 to 10.26) due to the pH of the thiol(s) stock solutions. The final pH was measured and was used to calculate the concentration of the negative form of the thiol, [RS^-], used in the plot k_ψ vs [RS^-] to calculate k_2^w. All reactions were performed at 30 °C.

2.5. Kinetics in the presence of CTAC

Stock solutions (0.001 M) of 4-nitro-NEHN in acetonitrile and 4-nitro-NBN in methanol were prepared. The stock solution (0.01 M) of HCys

was prepared in methanol and that of GSH and Cys in water. Kinetics were performed under pseudo-first order conditions. The concentration of the nitro-naphthalimides were usually 5×10^{-6} M and that of the thiols 5×10^{-5} M. All reactions were followed for, at least, 5 half-lives and the rate constants were obtained from linear first-order plots.

2.6. Stopped flow kinetics

The reaction of GSH and 4-nitro-NEHN, at pH 7.83, was followed in an Applied Photophysics Stopped-flow. The optical path of the cell was 0.2 cm. The two solutions (**a**) and (**b**) contained:

(a) Tris/HCl buffer, 0.01M, pH 8.0, CTAC at the desired concentration and 4-nitro-NEHN, and solution;
(b) HCl 0.001 M, CTAC at the same concentration of solution (**a**) and GSH at a concentration 10-fold that of 4-nitro-NEHN. The final concentration of 4-nitro-NEHN was 5×10^{-6} M and GSH 5×10^{-5} M.

The two solutions with identical volumes were mixed in the cell, and the final pH reduced from 8.0 to 7.83, due to the HCl content of solution (**b**). The rate constants are averages of three experiments with the same solutions.

2.7. Standard curves for the determination of SH groups concentrations of Cys, GSH, HCys and PRDX2, in CTAC

For quantitative determination of SH groups, both 4-nitro-NBN and 4-nitro-NEHN were used in excess. In a typical experiment, 10 μL of a 10 mM solution of naphthalimide (4-nitro-NBN in methanol and 4-NEHN in acetonitrile), to yield a final concentration of 250 μM of the probe, were added to 0.4 mL of buffer (in general Tris/HCl 0.01 M pH 7.5) containing CTAC 5 mM. To this solution a thiol aliquot was added at concentrations, at least, five times lower than the concentration of the naphthalimide. Fluorescence measurements were performed in a Hitachi F-2000 spectrofluorimeter at 700 V.

For quantitative determination of the SH contents of PRDX2, after stabilization of the fluorescence, the emission intensity was determined in the plate reader Fluorimeter using, for 4-nitro-NBN, $\lambda_{exc} = 390$ nm and $\lambda_{em} = 463$ nm and for 4-nitro-EHN, $\lambda_{exc} = 400$ nm and $\lambda_{em} = 487$ nm at 700 V. A plate reader Synergy H1 Hybrid Reader from Biotec was used to determine fluorescent intensity. All experiments were repeated three times, except for PRDX2 that was done induplicate.

n-Hexadecyl-cysteinamide chloride (HCys) and 4-Nitro-*N*-butyl-1,8-naphthalimide (4-nitro-NBN) were synthesized as described previously [15, 20].

2.8. Syntheses of 4-Nitro-N-ethylene-N, N′-dimethyl,N″-hexadecylammonium-1,8-naphthalimide bromide (4-nitro-NEHN)

4-nitro-NEHN was synthesized following the steps of previous synthesis of a similar compound [21]. Initially, 4-Nitro-1,8-naphthalic anhydride (2 mmol) and N,N-dimethyl-ethylenediamine (2.2 mmol) were mixed in 20 mL of ethanol under stirring at 50 °C and, after 10 min, 20 mL of water was added to the ethanolic solution forming a heterogeneous phase which was further sonicated in an ultrasonic bath (Bransonic 2510R-DTH Powerful Ultra) for 2 h. At the end, the product was filtered, washed with 50 mL of distilled water, and dried in an oven at 70 °C and the 4-nitro-N-ethylene-N,N′-dimethylamine-1, 8-naphthalimide was produced in a 80 % yield. The product was reacted with n-hexadecyl bromide, in a 1: 2.5 M ratio, in acetonitrile (20 mL) under reflux for 6 h. After cooling, 40 mL of diethyl ether was added forming a massive precipitate which was filtered, washed with 10 mL of diethyl ether, and dried in an oven at 70 °C yielding 90 % of 4-Nitro-NEHN.

Electrospray ionization mass spectrometry of 4-nitro-NEHN was obtained in a Quattro II Micromass mass spectrometer with Z-spray™ ion source (Manchester, UK), by direct injection, providing the expected molecular mass of the product, ESI^+ 538.3 m/z (Figure 1).

The ^{1}H NMR of 4-nitro-NEHN was recorded in a Bruker Avance III, 500 MHz spectrometer (Figure 2). ^{1}H NMR (500 MHz, CD_3OD, TMS) δ (ppm): 0.88 (t, 3H, $J = 7$ Hz); 1.27 (m, 22H); 1.42 (m, 4H); 1.88 (s, 2H); 3.27 (s, 6H); 3.50 (m, 2H); 3.66 (t, 2H, $J = 7,5$ Hz); 4.60 (t, 2H, $J = 7,5$ Hz); 8.07 (t, 1H, $J = 8$ Hz); 8.49 (d, 1H, $J = 8$Hz); 8.72 (d, 1H, $J = 8$ Hz); 8.74 (d, 1H, $J = 7,5$ Hz); 8.79 (d, 1H, $J = 8,5$ Hz).

The ^{13}C NMR of 4-nitro-NEHN (Brucker Avance III, 125 MHz, CD_3OD, TMS) is in Figure 3 and have the following signals: δ (ppm): 13.0; 22.1; 22.3; 25.9; 28.8; 29.0; 29.1; 29.2; 29.3; 29.3; 29.4; 31.6; 33.6; 48.4; 50.6; 59.2; 64.1; 122.6; 123.5; 123.6; 126.2; 129.0; 129.3; 129.6; 129.9; 132.1; 150.2; 162.6; 163.4.

The FTIR spectrum was recorded in a Bruker Alpha (KBr optics and DTGS detector) in the absorbance mode, using a Platinum ATR single reflection diamond ATR accessory, between 400 and 4000 cm^{-1} and spectral resolution of 4 cm^{-1} (Figure 4). The spectrum shown in Figure 4 was the result of the coaddition of 256 individual spectra. FTIR, υ (cm^{-1}): 3066, 2920, 2850, 1708, 1665, 1527.

2.9. Evidencing SH groups in living cells

Human leukemia cells line HL-60 and THP-1 were cultured in RPMI-1640 medium supplemented with penicillin (100 U/mL), streptomycin (100 μg/mL), 20% FBS (fetal bovine serum) and maintained in an atmosphere of 5% CO_2 at 37 °C. Cells were differentiated in neutrophils (dHL-60) with 1.3% DMSO (dimethyl sulfoxide) for 4 days or in macrophages (dTHP-1) with 5 ng/mL PMA (phorbol 12-myristate 13-acetate) for 2 days in growth medium supplemented with 10% FBS. Cells (5×10^6 dHL-60 or 2×10^6 dTHP-1 for each group) were washed with phosphate buffer saline (PBS) supplemented with glucose (10 mM Na_2HPO_4; 2 mM KH_2PO_4; 137 mM NaCl, 1 mM $CaCl_2$, 0.5 mM $MgCl_2$ and 1 g/L glucose, pH 7.4) for dHL-60 or PBS with no glucose, for dTHP-1, and incubated in the same buffer at 37 °C with: A) only PBS; B) 100 μM 4-NBN for 30 min; C) pre-incubated with 5 mM hydrogen peroxide for 15 min, washed and incubated with 100 μM 4-NBN for 30 min or D) pre-incubated with 100 μM 4-NBN for 30 min, washed and incubated with 5 mM hydrogen peroxide for 15 min. The groups were analyzed in the fluorescence microscopy Nikon Eclipse TE300 (40 x objective lens). The excitation was at UV light and fluorescence emission was detected using a blue filter.

3. Results and discussion

Cys and GSH reacted with 4-nitro-NBN (maximum wavelength, λ_{max} = 353 nm in water), displacing the nitro group (Scheme 1), yielding products with maximum absorption wavelengths (λ_{max}) at 380 and 378 nm, respectively (Figure 5, Table 1). The structures of the products of similar reactions of 4-nitro-NBN with aromatic and aliphatic thiols are known [14]. The spectra of the products of 4-nitro-NBN with Cys (Figure 5A) and GSH (Figure 5B) showed a displacement of the maximum wavelength for both reactions as a function of time (Figure 5, Table 1). The thiols were in high excess over the 4-nitro-naphthalimide due to the slow rate of the reactions in water. The observed rate constants (k^0_ψ) of the reaction of thiols with 4-nitro-NBN depended linearly of the concentration of negatively charged species of Cys, [Cys^-], and GSH, [GSH^-] (Figure 5C). From the slope of the plots of Figure 5C, the second-order rate constants for each thiol (k^0_2) were obtained (Eq. 2).

$$k^0_w = k^0_2 x[Cys^-] \quad (2)$$

The concentration of [Cys^-] was calculated using a pK_a of 8.65, and that of GS^- using a pK_a of 9.6 for GSH, determined in this work, see below [4, 25]. The k^0_2, for the reactions of Cys^- and GS^- with 4-nitro-NBN were 27.8 $M^{-1}min^{-1}$ and 65.2 $M^{-1}min^{-1}$, respectively.

The reactions in the aqueous phase, under pseudo-first-order conditions, even at high concentration of Cys and GSH with the nitro-naphthalimides, were relatively slow, and thiol oxidation may compete with NO_2 substitution under these conditions [26]. Micelles are convenient systems to increase bimolecular reaction rates, in particular those where the nucleophile is the anion of a weak acid [20].

The quantitative analysis of reactions in the micellar phase of a nucleophile derived from the dissociation of a weak acid, such as a thiol, must consider the effect of the micelles on the apparent dissociation constant of the acid [27]. Therefore, we first determined the values of the apparent pK_a, pK_{ap}, of Cys, HCys and GSH, as a function of CTAC concentration, [CTAC] (Figure 6). The pK_{ap} of all thiols decreased with the increase of [CTAC] reaching a minimum value and increased with higher [CTAC] (Figure 6A, B, C). The effect of [CTAC] on the pK_{ap}'s of the thiols reflects at least two factors: a) the differences their hydrophobicity, which leads to the different association degree with the micelles, and b) the relative efficiency of the binding of the dissociated (negatively charged) thiol to the positive CTAC and its exchange with other anions presents at the micellar surface.

The pK_a of HCys in water was determined by extrapolation of the plot of Figure 6A to zero [CTAC] ($pK_a = 8.5$). For Cys, the pK_a calculated by extrapolation of the plot of Figure 7B ($pK_a = 8.65$), was similar to published values ($pK_a = 8.53$) [3]. Benesh et Benesh attributed a $pK_a = 8.53$ for the –SH group of Cys to the [$-S^-/NH_3^+$] form and a $pK_a = 10.03$ for the [$-S^-/NH_2$] form of Cys [3, 4]. The pK_a of GSH's thiol in water, determined here, was 9.6 (Figure 2C, inset), in good agreement with the data of [25] ($pK_a = 9.42$ +/- 0.17) but higher than the data of Benesch [3] ($pK_a = 9.2$).

The experimental data on Figure 6 were fitted to Eq. (3) [16], where A and AH refer to the anionic and the protonated form of the thiol. The sub-index *f* and *b* refer to ions, or substrates, free in aqueous phase and bound to micelles, respectively.

In Eqs. (4), (5), and (6), K_{HA} is the micelle/water distribution constant of the protonated thiol (Eq. 4), $K_{A/Cl}$ is the thiol anion/chloride exchange constant (Eq. 5), $K_{OH/Cl}$ and $K_{OH/A}$ are hydroxide/chloride and hydroxide/thiol anion exchange constants respectively. C_D is the concentration of micellized surfactant is given by Eq. (6), where CT is the total detergent concentration and cmc is the critical micellar concentration. Eqs. (7) and (8) allow the calculations of [Cl_f], [Cl_b] and [OH_b]. In Eq. (7), [Cl_{AD}] refers to the concentration of added Cl from a salt or buffer.

$$K_{ap} = K_a \frac{1 + K_{A/Cl}\left(Cl_b / Cl_f\right)}{1 + K_{HA} C_D} \tag{3}$$

$$K_{HA} = \frac{[HA_b]}{[HA_f] x C_D} \tag{4}$$

$$K_{A/Cl} = \frac{[A_b][Cl_f]}{[A_f][Cl_b]} \quad or \quad K_{OH/Cl}/K_{OH/A} \tag{5}$$

$$C_D = C_T - cmc \tag{6}$$

$$\left[Cl_f\right] = \alpha C_D + [A_b] + [OH_b] + [Cl_{AD}] \tag{7}$$

$$[Cl_b] = (1 - \alpha C_D) - [OH_b] - [A_b] \tag{8}$$

In the analysis, we considered that the affinity of the anions of the buffers to CTAC, were like that of Cl^-. The concentration of the anionic form of all buffers were included in the simulation as equal to [Cl_{AD}]. The concentration of the anionic form of the buffers, at different pHs, were calculated using the following pK_a's ($pK_a^{MES} = 6.15$, $pK_a^{TRIS} = 8.1$, $pK_a^{HEPES} = 7.5$) and the buffer concentration.

The lines in Figure 6, and those of kinetic data, were obtained using $\alpha = 0.27$ and $K_{OH/Cl} = 0.14$ [27]. The cmc's were different for each experimental condition and used as an adjustable parameter. K_{AH}, $K_{A/Cl}$ and $K_{OH/A}$ were obtained from the fit of the pK_{ap} curves using Eqs. (3), (4), (5), (6), (7), and (8).

For Cys, the best fit values were: $K_{OH/A} = 0.2$ and $K_{HA} = 5\ M^{-1}$ and for HCys, $K_{OH/A} = 8 \times 10^{-4}$ and $K_{HA} = 1.0 \times 10^4\ M^{-1}$. For GSH the values of $K_{OH/A} = 0.006$ and $K_{HA} = 150\ M^{-1}$ were used.

The exchange of GS^- by Cl and OH at the micellar surface is clear in the data in Figure 6D. Increasing [NaCl] led to the increase in the pK_{ap} of GSH (Figure 6D), indicating that added Cl displaced both OH^- and GS^- from the micelle, leading to a decrease in the pH at the micellar surface.

The effect of [CTAC] on the observed pseudo-first order rate constants (k_ψ) of the reactions of Cys with 4-Nitro-NBN and 4-Nitro-NEHN are in Figures 7A and 7B, respectively. k_ψ increased with micelle concentration, reaching a maximum (k_ψ^{max}) at [CTAC] ca. 2×10^{-3} M and decreasing at higher concentrations. The maximum acceleration of the CTAC micelles was calculated by the ratio k_ψ^{max}/k_ψ^0, where k_ψ^0 is the observed rate constant of the reactions in the same buffer without micelles. The values of k_ψ^0 were calculated with Eq. (2) using the $k_2^0 = 27.8\ min^{-1}$ for both the reaction of Cys with 4-Nitro-NBN and 4-Nitro-NEHN and a $pK_a = 8.65$ for Cys. The ratio k_ψ^{max}/k_ψ^0 was ca. 3,500 for the reaction of Cys with 4-Nitro-NEHN (at pH's 7.5 and 8.0) and ca. 750 with 4-Nitro-NBN, at pH 8.5, Table 2.

Experimental kinetic data in Figure 7 were fitted using Eq. (9) [16] where k_2^m is the second-order rate constants in the micellar phase and H_f is the proton concentration in the buffered bulk solution. [HA] is the total concentration of the thiol used in the experiment and V is the molar volume of the micellized CTAC which has a value of 0.32 l/mol [27]. K_S, the association constant of the nitro-naphthalimides with the micelles, is given by Eq. (10), where S_b and S_f are the analytical concentration of bound and free nitro-naphthalimide, respectively [20].

$$k_\psi = [HA] K_a \frac{\left(k_2^m / V\right)\left(K_s K_{A/Cl}\right)\left(Cl_b / Cl_f\right) + k_2^0}{(1 + K_{HA} C_D)\left(\left[H_f\right] + K_{ap}\right)(1 + K_S C_D)} \tag{9}$$

$$K_S = \frac{S_b}{[S_f] x C_D} \tag{10}$$

The values of K_S for 4-Nitro-NBN and 4-Nitro-NEHN, and $K_{OH/A}$ and

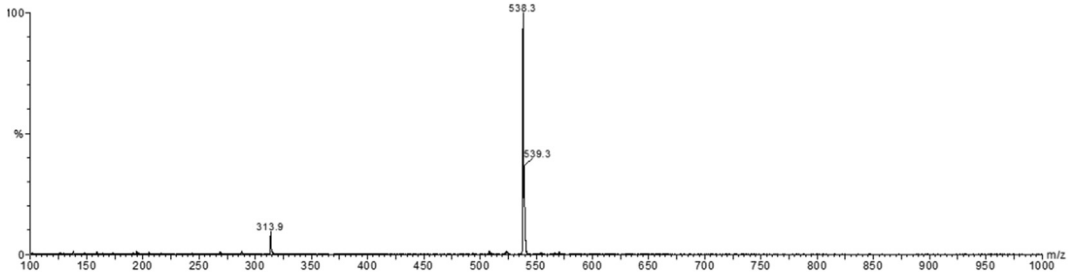

Figure 1. Mass Spectrum of 4-nitro-1,8-naphthalimide-N-ethylene-N, N′-dimethyl, N″-hexadecyl bromide, ESI^+ 538.3 m/z.

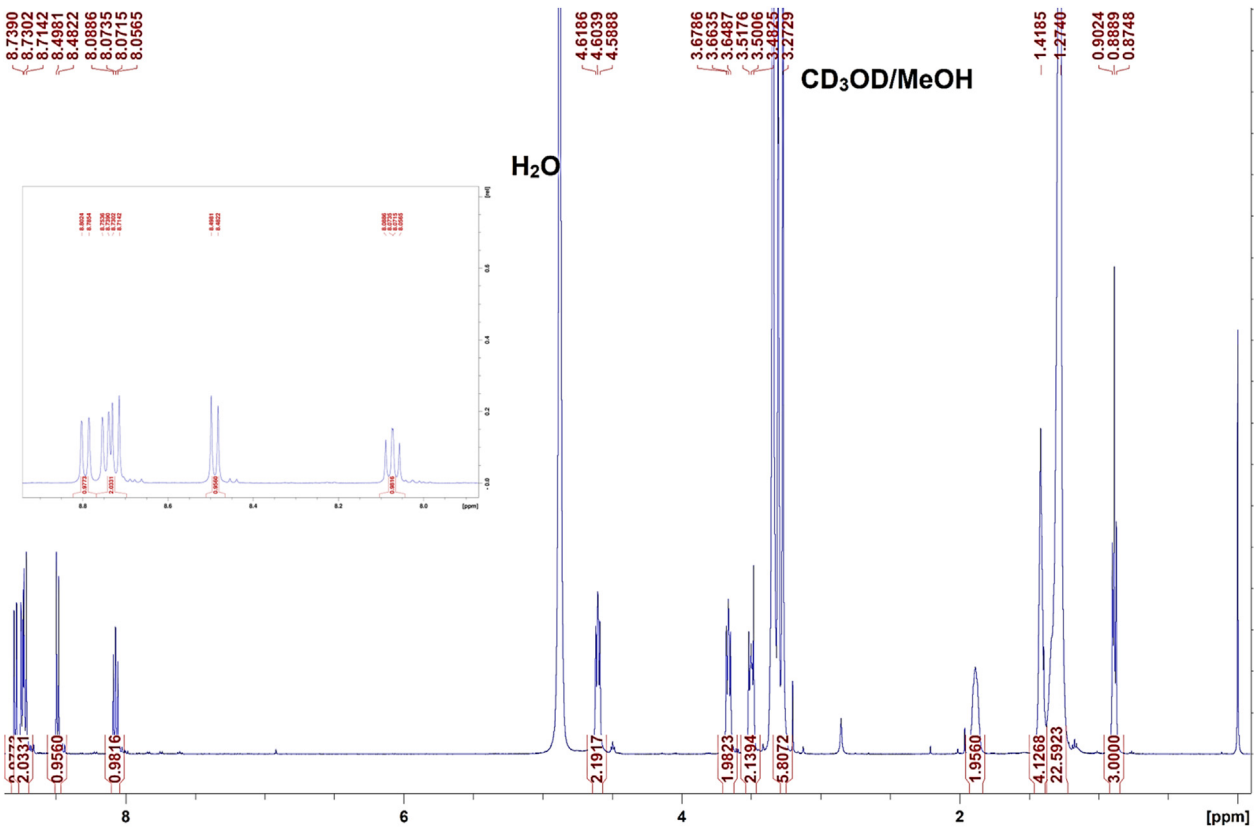

Figure 2. - ^{1}H NMR of 4-nitro-1,8-naphthalimide-N-ethylene-N, N′-dimethyl, N″-hexadecyl bromide (500 MHz, CD_3OD, TMS) δ (ppm): A) complete spectrum. B) Expansion of the 7.5–9.0 ppm region.

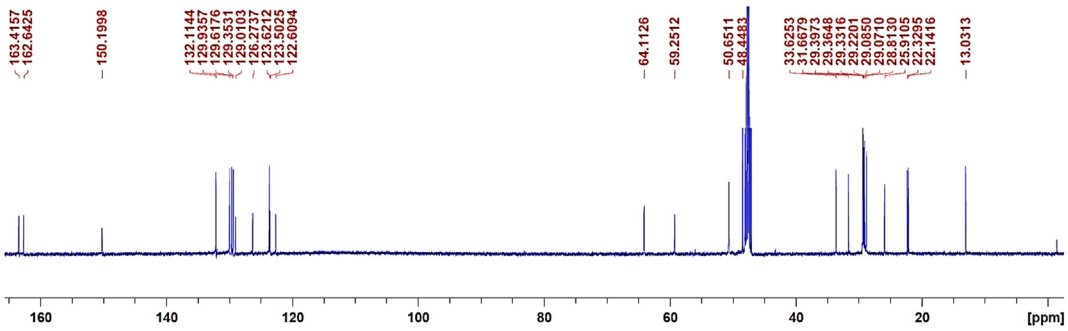

Figure 3. ^{13}C NMR of 4-nitro-1,8-naphthalimide-N-ethylene-N, N′-dimethyl, N″-hexadecyl bromide (125 MHz, CD_3OD, TMS) δ (ppm).

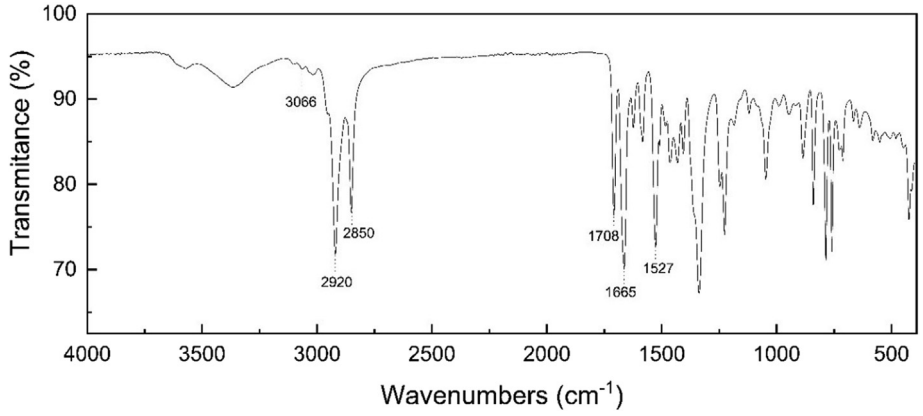

Figure 4. FTIR of 4-nitro-1,8-naphthalimide-N-ethylene-N, N′-dimethyl, N″-hexadecyl bromide.

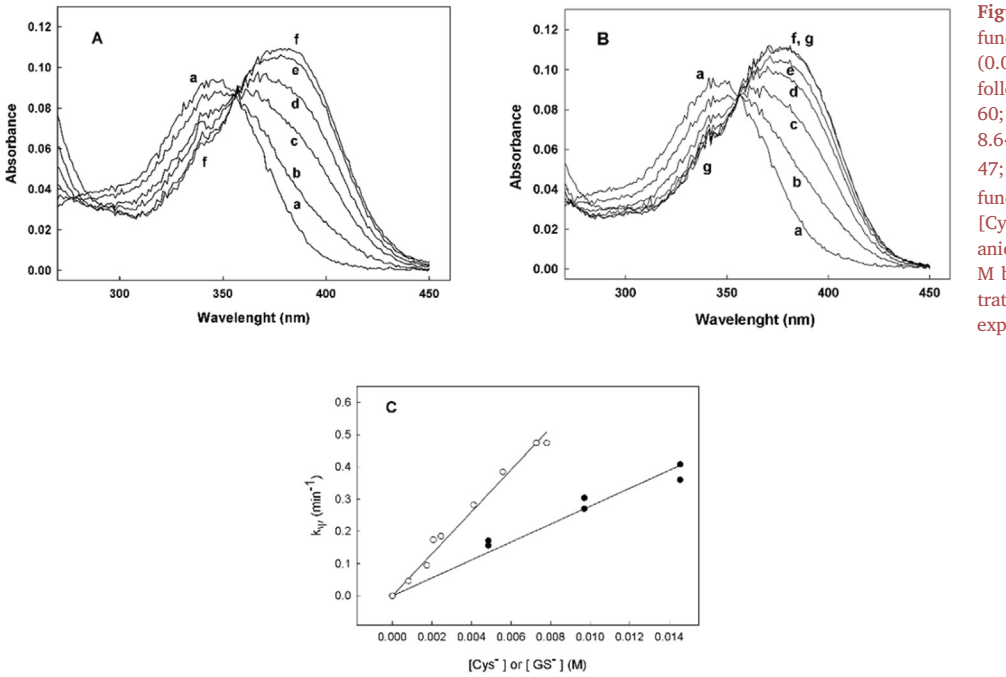

Figure 5. Spectra of the reaction product(s), as a function of time, of 4-nitro-NBN with: (A) Cys (0.01 M) in Tris/HCl 0.1 M, pH 8.23 buffer, at the following times (min): a) 0; b) 10; c) 30; d) 40; e) 60; f) 68. B) GSH (0.01 M) in Tris/HCl 0.1 M, pH 8.64; times (min): a) 0; b) 4; c) 10; d) 19; e) 27; f) 47; g) 67. C) Observed rate constants (k_ψ^0) as a function of the anionic concentration of Cys, [Cys$^-$], in borate buffer 0.15 M pH 10.0 (●) and anionic form of glutathione [GS$^-$] in CAPSO 0.15 M buffer, at initial pH of 10.6 (◯). The concentration of 4-nitro-NBN was 8.9 × 10^{-6} M in all experiments.

Table 1. Maximum Absorption Wavelength, λ, and Molar Extinction Coefficients, ε, of the products of the reactions between 4- nitro-naphthalimides and the thiols, in water and CTAC. The excitation, λ_{exc}, and emission, λ_{em}, wavelengths of the products of the reactions of 4-nitro-NEHN and 4-NBN with GSH, HCys and PRDX2 are given. [CTAC] = 1.0 mM.

Naphthalimide	Thiol	Products, λ_{max} (nm); ε (M.cm^{-1})	λ_{exc} (nm)	λ_{em} (nm)
4-Nitro-NBN	Cys (buffer)	380		
	GSH (buffer)	378		
	Cys (CTAC)	390	390	463
	HCys (CTAC)	379; (11,521)	390	463
	GSH (CTAC)	377; (10,022)	390	476
	PRDX2 (CTAC)	390	390	461
4-Nitro-NEHN	Cys (CTAC)	400	400	487
	GSH (CTAC)	400; (11,667)	400	470
	HCys (CTAC)	400; (11,850)	400	478
	PRDX2 (CTAC)	390	390	479

K_{AH} used in each simulation are in the legend of Table 2. The K_S of 4-Nitro-NBN used here is in accord with already experimentally determined value and was 1,877 M^{-1} [15].

The k_2^m/k_2^0 ratio for the reaction of Cys with 4-Nitro-NBN and 4-Nitro-NEHN were ~4 and ~15 respectively, while the maximum acceleration factors are between 760 and 3.5 × 10^3, respectively (Table 2). These values indicate that the micellar effects were strongly dependent on the hydrophobicity of the Nitro-naphthalimide, and that the major factor of acceleration is due to the concentration of the substrates at the micellar interface. The k_{2m}/k_{20} ratio was low for the two reactions, thus the intrinsic reactivity did not change significantly when compared with the reaction in water.

CTAC micelles also increased the reaction rate of 4-nitro-NBN with GSH and HCys (Figure 8). A time dependent change of the spectrum and a displacement of the maximum absorption wavelength were observed with both thiols due to the formation of the products RS-NBN (Scheme 1) (Figure 8). The products of 4-nitro-NBN with HCys and GSH had an absorption maximum at 379 and 377 nm, respectively (Table 1).

The UV spectra of 4-nitro-NBN in CTAC has a maximum at 353 nm and the reaction with HCys (Figure 9) displaces the maximum absorption wavelength to 379 and with GSH to 377 nm (Table 1) due to 4-RS-NBN formation of (Scheme 1).

CTAC micelles catalyzed the reactions of 4-nitro-NBN with GSH and HCys at different pH's (Figure 9) and the shapes of the plots of k_ψ vs [CTAC] were similar to those shown in Figure 7. The effect of [CTAC] on k_ψ in the reaction of 4-nitro-NBN with GSH was determined in Tris/HCl buffer, 0.01 M, at pH 7.5 (Figure 10A). In Figure 5B are the rate constants of the same reaction in Tris/HCl, 0.01M, pH 7.10, and in MES 0.01 M, pH 7.11. The concentration of Cl in Tris/HCl 0.01 M, pH 7.1 buffer is 9 mM (Tris pK_a = 8.1) and that of the anionic form of MES 0.01 M, pH 7.1 is also 9 mM (MES pK_a is 6.1). In spite of the differences in the buffer composition the data in Figure 5B were very similar, indicating that the ion-exchange constant between OH and Cl ($K_{OH/Cl}$) and OH and MES ($K_{OH/MES}$) are essentially identical.

The high values of k_ψ^{max}/k_ψ^0, in the reaction of 4-NBN with GSH, were not comparable to the small k_2^m/k_2^0 (see Table 2), indicating a small

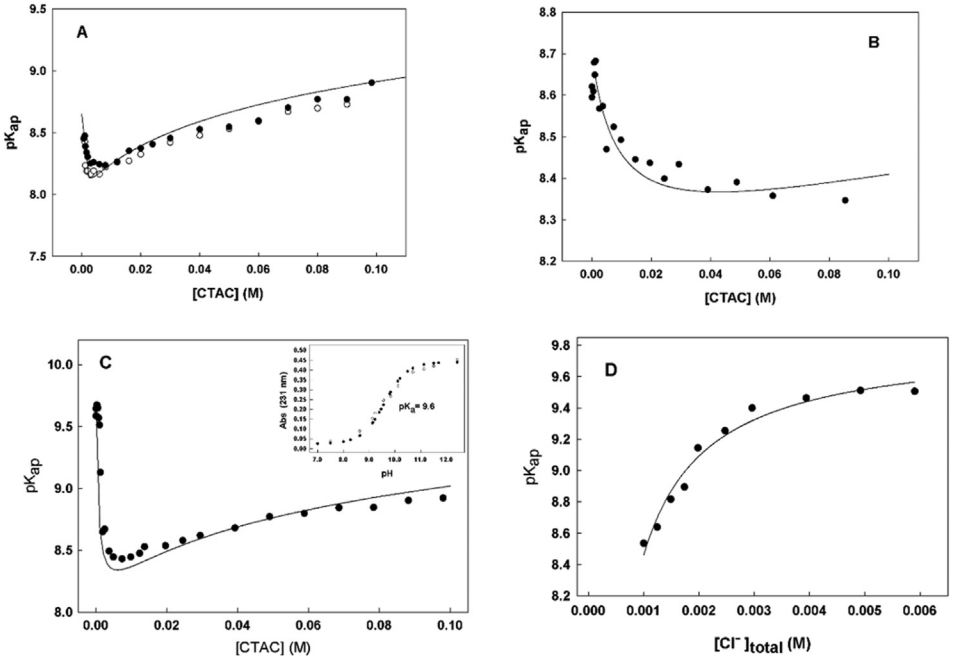

Figure 6. Effect of [CTAC] on the pK_{ap} of: A) HCys, Tris/HCl 0.01 M pH 8.53, [HCys] = 4.58×10^{-5} M. B) Cys in Tris/HCl 0.01 M pH 8.5, [Cys] = 5.82×10^{-5} M. C) GSH, Tris/HCl buffer, 0.01 M, pH 9.05, [GSH] = 4.8×10^{-5} M. Inset-Absorbance of GSH at 231 nm as a function of pH 6.1×10^{-5} M (D) Effect of [NaCl] in the pK_{ap} of GSH, at [CTAC] = 0.008 M and [GSH] = 5×10^{-5} M, Tris/HCl buffer, 0.01 M, pH 9.05. In all experiments [TCEP] = 1×10^{-4} M. Symbols are experimental points and lines (A, B and C) were calculated using Eqs. (3), (4), (5), (6), (7), and (8).

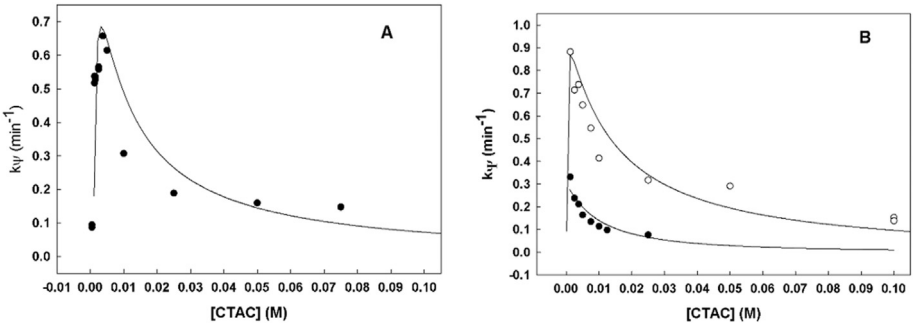

Figure 7. Effect of [CTAC] on the rate constants of the reactions of Cys with: A) 4-Nitro-NBN in TRIS/HCl buffer 0.01 M, pH 8.5, [4-nitro-NBN] = 3.72×10^{-6} M and [Cys] = 5.53×10^{-5} M. B) 4-nitro-NEHN in HEPES buffer, 0.01 M, pH 7.5 and ((●)TRIS/HCl pH 8.0, [4-nitro-NEHN] = 4.15×10^{-6} M, [Cys] = 4.9×10^{-5} M (◯).

difference in the reactivity of the GSH thiol in the micelle interface in comparison with water.

The reaction of HCys with 4-nitro-NBN in CTAC, in MES buffer, pH 5.52 (Figure 10C), reached $k_{\psi}^{max}/k_{\psi}^{0} = 2.5 \times 10^{6}$, and a calculated k_2^m/k_2^0 near 83, indicating that, with this more hydrophobic thiol, the reaction site was different from that of GSH (Table 2).

The reaction of HCys and 4-nitro-NEHN in [CTAC] was studied at pH 5.54 and the value of $k_{\psi}^{max}/k_{\psi}^{0}$ was ca. 2.5×10^{7}, the highest acceleration factor obtained, and k_2^m/k_2^0 was ca. 720 (Figure 10A, Table 2). Increasing [NaCl] in the reaction at fixed [CTAC] (MES buffer, 0.01 M, pH 5.54) (inset Figure 11) led to a decrease of k_{ψ}. as expected for a bimolecular reaction in micelles which depends on the [OH] for the nucleophile dissociation [16].

CTAC increased the rate of the reaction between GSH and 4-nitro-NEHN at pH 5.12, with a $k_{\psi}^{max}/k_{\psi}^{0}$ of 2.98×10^{6} (Figure 10, Table 2). The calculated k_2^m/k_2^0 ratio was the highest for all reactions described here, an increase in intrinsic reactivity of ca. 10^3. The reactions at pH 7.83 were faster than those described previously and CTAC produced a significant rate acceleration, $k_{\psi}^{max}/k_{\psi}^{0} = 6.4 \times 10^{5}$ (Figure 10C, Table 2).

The values of $k_{\psi}^{max}/k_{\psi}^{0}$ varied from ca. 750 to 2.5×10^{7}, depended on the hydrophobicity of the nitro-naphthalimides and of the thiols, pH and salt concentration. Micelle acceleration of these reaction can, as will be shown below, be used to detect and quantify SH groups of different biological thiols. To improve the analytical use of these nitro-naphthalimide, we studied the fluorescence properties of the products of these reactions in different conditions [15].

3.1. Fluorescence of the products of the reactions of thiols and nitro-Naphthalimides

The products of the reactions of nitro-naphthalimides with thiols are fluorescent [15] and this property was used to quantify protein SH groups. The maximum absorption wavelength of the reaction products of 4-nitro-NBN and 4-nitro-EHN with different thiols were in the range of 377 and 400 nm (Table 1) and the emission fluorescence, λ_{em}, of products were between 460 nm and 480 nm.

In Figure 11 are the fluorescence spectra of the products of the reactions of 4-nitro-NBN and 4-nitro-NEHN with HCys and GSH in CTAC, as a function of time, at pHs 5.5 and 7.5. The fluorescence spectra and the maximum emission wavelength are similar for all products (Table 1). The pH and the nitro-naphthalimide can be selected to minimize the thiol

oxidation during the analysis. Independent of the pH used, the reactions of HCys or GSH with 4-nitro-NEHN are faster than that with 4-Nitro-NBN (Figure 11A, B).

3.2. Using 4-nitro-naphthalimides for thiol determination in excess of naphthalimide

To determine thiol concentrations we used an excess, ca five-fold of -nitro-NBN and 4-nitro-NEHN. The time for complete reaction depended on the thiol structure and pH, and varied from minutes to 1 h. In the case of Cys and GSH, the reactions were performed at pHs 7.5 to 8.0, but, for more hydrophobic thiols and for proteins, pHs as low as 5.5 can be used. The fluorescence intensity dependence of the products of the reaction of 4-NBN or 4-nitro-NEHN with different thiols in CTAC are in Figure 12.

Standard curves for HCys and GSH (Figure 12) in CTAC were obtained using 4-NBN and 4-nitro-NEHN ($\sim 2 \times 10^{-5}$ M) in 0.01 M MES buffer, pH 6.5, and in 0.01 M Tris/HCl pH 7.5, respectively. Experiments were done in triplicate and the standard deviation are in Figure 12. Correlation coefficients and slopes are in the legend of Figure 12. Fluorescence intensities were obtained after complete reaction, i.e., fluorescence stabilization.

For Cys, as the reaction is relatively slow, pH used was 8.0 and the time to complete the reaction was 1 h. With both naphthalimides, the standard curves were linear up to 14 μM Cys. The lower detection limit for Cys was in the μM range.

In the reaction of thiols with DTNB, the presence of an oxidant, such a H_2O_2, re-oxidizes the reaction product (TNB) preventing the use of DTNB as a tool for SH quantifications. Addition of H_2O_2, however, did not affect the product in this method.

The effect of H_2O_2 on the absorption spectra of 4-Nitro-NBN and of the product of the reactions with thiols was determined as follows. The absorption spectra of 4-Nitro-NBN (6.25×10^{-5} M) in CTAC (4 mM) Tris-HCl 0.01 M, pH 7.5 was unaffected by the addition of 4 mM H_2O_2. The absorbance spectrum 4-Nitro-NBN, under the same conditions described above, was taken, and then GSH (1.1×10^{-4} M) was added. After complete reaction, i.e., absorbance stabilization, subsequent addition of 4 mM of H_2O_2 (final concentration) produced no spectral change, indicating that the product was stable in this oxidant condition.

For both probes and thiols, the products fluorescence values were linear from 1×10^{-6} M up to 5×10^{-6} M of thiol. In the classic method using DTNB, the lower detection limit is of the order of 5×10^{-6} M [17].

3.3. Using 4-Nitro-naphthalimides to measure PRDX2 SH groups

PRDX2 is an enzyme containing three SH groups [28]. Fast reactions of PRDX2, with nitro-naphtalimides, were observed at pH 7.5 with CTAC (5 mM). Fluorescence increased with a maximum at 462 nm and 470 nm for 4-nitro-NBN and 4-nitro-NEHN, respectively, as obtained with GSH and HCys (Table 1). The fluorescence spectra of the products of PRDX2 with 4-Nitro-NBN and 4-Nitro-NEHN at the end of the reaction (5 min) as a function of PRX2 concentration, are shown in Figure 13 A, B. The relative fluorescence intensity was linearly dependent on [PRDX2] (Figure 13C) for both naphthalimides. The sensitivity of the method allows the detection of the SH groups in PRDX2 using 1×10^{-7} M of enzyme.

3.4. 4-nitro-NBN and 4-nitro-NEHN as potential probes for fluorescent imaging: oxidant conditions

The use of the 4-nitro-NBN and 4-nitro-NEHN as potential probes to detect intracellular thiols was explored in living cells by fluorescent imaging. Human leukemic cells, HL-60, and THP-1 monocytes line cells were respectively differentiated into neutrophil-like and macrophages and then incubated at 37 °C in PBS/glucose and 100 μM 4-nitro-NBN for 30 min. No fluorescence was detected in the absence of 4-nitro-NBN but a high fluorescence was detected after incubation with 4-nitro-NBN (Figure 14). The addition of 5 mM H_2O_2 to the cells for 15 min, after the incubation with 4-nitro-NBN, does not decrease the fluorescence. Cells pre-incubated with 5 mM hydrogen peroxide (15 min), washed and then incubated with 100 μM 4-nitro-NBN for 30 min, exhibited a significant decrease in fluorescence. Nitro-naphthalimides are also substrates to nitro-reductases yielding fluorescent products [29]. However, the formation of the two-electron reduced fluorescent products from nitro-naphthalimides by nitro-reductases is relevant only in hypoxic conditions since, in presence of oxygen, a one-electron redox reaction with formation of non-fluorescent products takes place [29, 30].

Table 2. Maximum first-order rate constants, k_ψ^{max}, in CTAC, obtained from data in the Figures, calculated first-order rate constants in water, k_ψ^0, at the same pH and thiol concentration for each experiment, and calculated second-order rate micellar constant, k_m, used to fit the experimental data using the ion-exchange model.

Thiol	Buffer 0.01 M	pH	k_m (min^{-1})	k_m/k_o	k_ψ^{max} (min^{-1})	$^*k_\psi^0$ (min^{-1})	k_ψ^{max}/k_ψ^0
4-NBN							
GSH	**TRIS/HCl	7.83			35.0	5.44×10^{-5}	6.4×10^5
GSH	TRIS/HCl	7.11	350	5.4	0.156	1.0×10^{-5}	1.56×10^4
GSH	TRIS/HCl	7.50	500	7.7	0.624	2.57×10^{-5}	2.43×10^4
HCYS	MES	5.52	2,300	82.7	2.358	9.44×10^{-7}	2.5×10^6
CYS	TRIS/HCl	8.5	110	4.00	0.657	9.04×10^{-4}	756.8
16-NHEN							
GSH	MES	5.12	6.5×10^4	996.9	0.264	8.85×10^{-8}	2.98×10^6
GSH	MES	6.07	6700	102.8	0.60	8.35×10^{-7}	7.18×10^5
GSH	MES	6.53	5500	84.3	0.906	1.75×10^{-6}	5.18×10^5
GSH	TRIS/HCl	7.00	2,500	38.4	1.43	1.00e-5	1.43×10^5
HCYS	MES	5.54	2×10^4	719.4	24.06	9.62×10^{-7}	2.5×10^7
CYS	HEPES	7.5	450	16.2	0.331	9.02×10^{-5}	3.67×10^3
CYS	TRIS/HCl	8.0	400	14.4	0.882	2.5×10^{-4}	3.54×10^3

$^*k_\psi^0$ at each pH was calculated using the equation: $k_\psi^0 = [RS^-] \times k_2^0$. The values of $k_2^{GSH} = 65.2\ M^{-1}\ min^{-1}$; k_0^{CYS} and $k_0^{HCYS} = 27.8\ M^{-1}min^{-1}$ were used for both 4-nitro-NBN and 4- Nitro-NHEN. The $[RS^-]$ was calculated using the concentration of thiol and the pK_a^S: $pK_a^{GSH} = 9.6$; $pK_a^{CYS} = 8.65$ and $pK_w = 13.836$ (at t = 30 °C). The best fit values of the curves were obtained using the following constants: $K_{OH/Cl} = 0.14$, $K_{GS/Cl} = 23.3$, $K_{Cys/Cl} = 0.7$, $K_{HCYS/Cl} = 175$. The following parameters were used: $K_{HA}(GSH) = 150\ M^{-1}$; $K_{HA}(HCYS) = 1.1 \times 10^4\ M^{-1}$; $K_{HA}(Cys) = 5\ M^{-1}$ (except for curve of CYS and 16-NHEN, pH 7.5 where the best fit was obtained with $K_{HA}(Cys) = 60\ M^{-1}$). K_S (4-Nitro-NBN) = 1,877 M^{-1} and K_S (4-Nitro-NHEN) = $1 \times 10^4\ M^{-1}$. $K_{OH/Cys} = 0.2$; $K_{OH/GS} = 0.006$ and $K_{OH/HCYS} = 8 \times 10^{-4}$. **These experiments were performed in the stopped flow and the final concentration of Tris/HCl was 4 mM.

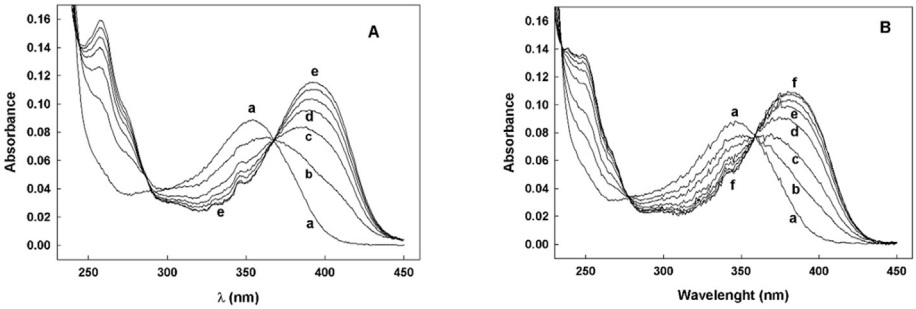

Figure 8. Spectra of the reaction mixtures of HCys and GSH with 4-nitro-NBN in CTAC in Tris/HCl 0.01M, pH = 7.0, as a function of time (min). A) HCys: a) t = 0; b) t = 0.5; c) t = 1.0; d) t = 1.5; e) t = 5. HCys = 5.27×10^{-5} M. B) GSH: a) t = 0; b) t = 2.5; c) t = 5; d) t = 10; e) 15; f) 30, GSH, 5×10^{-5} M. All reaction mixtures contained [CTAC] = 2×10^{-3} M and [4-nitro-NBN] = 8.2×10^{-6} M.

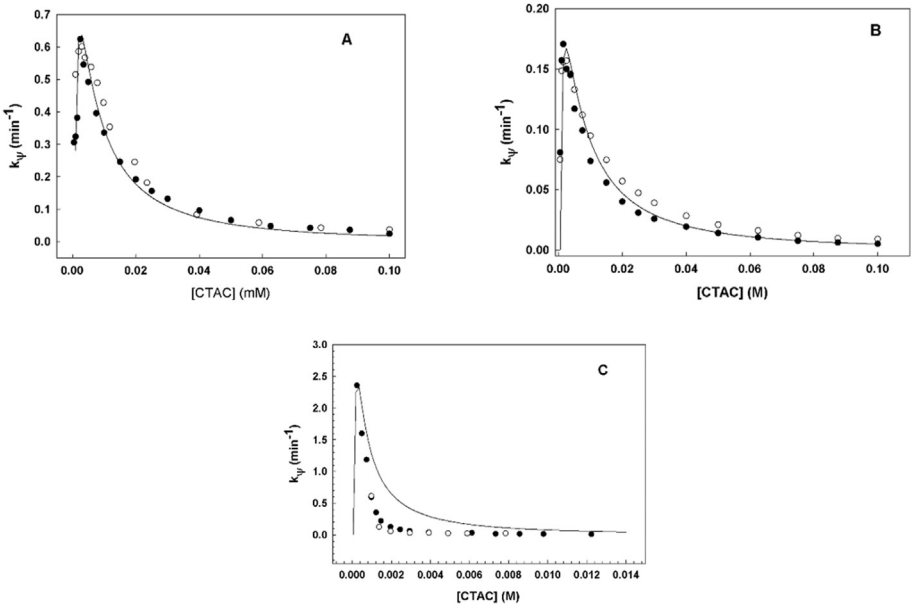

Figure 9. Effect of [CTAC] on the rate constant of the reaction of 4-nitro-NBN and thiols at different pHs. A) GSH in Tris/HCl 0.01M pH 7.5 buffer, [GSH] = 4.9×10^{-5} M (the symbols (●) and (○) are two independent sets of experiments. B) GSH in Tris/HCl 0.01M pH 7.11 buffer (○) and MES 0.01 M, pH 7.1 (●) [GSH] = 4.9×10^{-5} M. C) HCys in MES 0.01 M, pH 5.52 (●, ○) [HCYS] = 4.58×10^{-5} M. [4-nitro-NBN] = 3.92×10^{-6} M for all experiments. The symbols are experimental data and the lines are theoretical (see text).

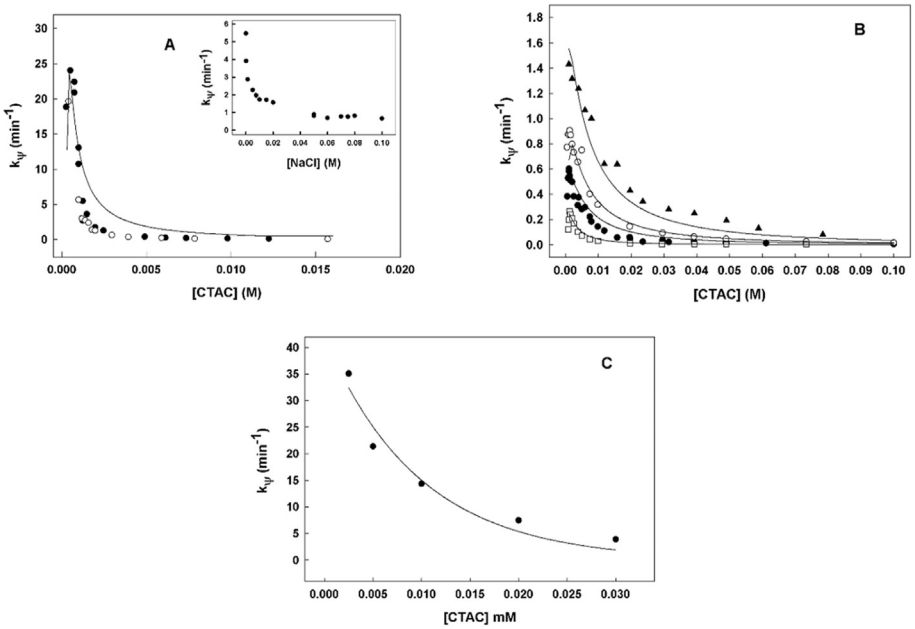

Figure 10. Effect of [CTAC] on the reaction rates of 4-nitro-NEHN with: A) HCys in MES buffer, 0.01 M, pH 5.54, [4-nitro-NEHN] = 4.15×10^{-6} M, [HCys] = 4.60×10^{-5} M. The symbols (◯) and (●) refers to two different sets of experiments. Insert shows the effect of NaCl concentration in the reaction rate at CTAC 1.2 mM at pH 5.54. B) GSH in MES buffer 0.01 M, pH 5.12 (□); pH 6.07 (●); pH 6.53 (◯) and T. Tris/HCl 0.01 M pH 7.0 (▲); The symbols are experimental data and the lines. [4-nitro-NEHN] = 3.72×10^{-6} and [GSH] = 4.8×10^{-5}. C) Effect of CTAC in the reaction of GSH and 4-nitro-NEHN in Tris/HCl 0.004 M, pH 7.83. The [4-nitro-NEHN] was 5×10^{-6} M and [GSH] was 5×10^{-5} M.

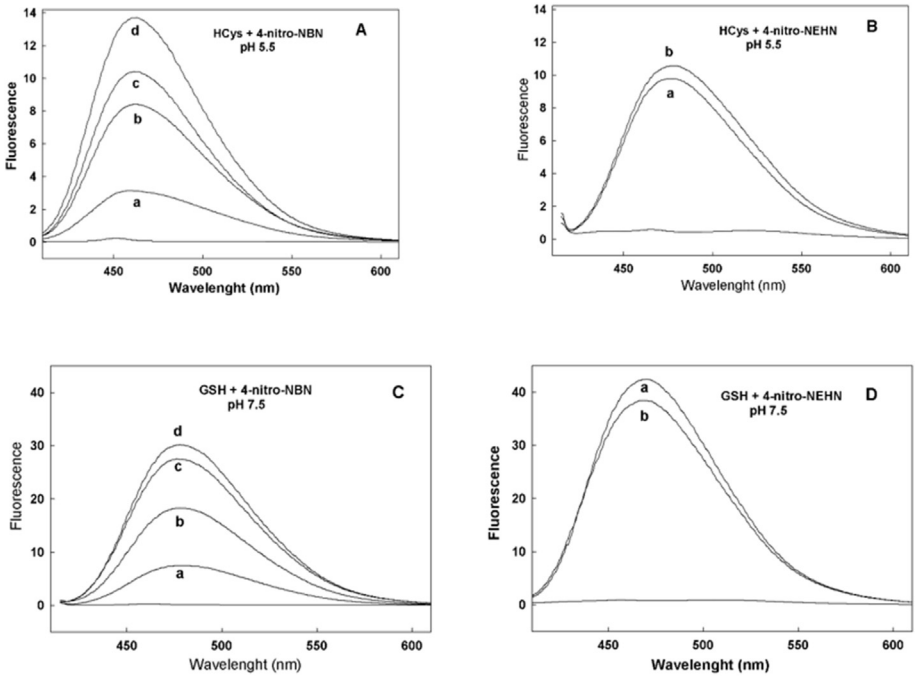

Figure 11. Emission fluorescence spectra of the reaction products of 4-nitro-NEHN and 4-nitro-NBN with HCys and GSH in CTAC as a function of time (min). (A) [HCys] = 4.6×10^{-5} M, [4-nitro-NBN] = 4.1×10^{-6} M, MES, 0.01 M, pH 5.5. Time (min): a) 0.5; b) 1.4; c) 3.6; d) After 10 min (B) [HCys] = 6.2×10^{-5} M, [4-nitro-NEHN] = 4.5×10^{-6} M, MES, 0.01 M, pH 5.5. Time (min): a) 0.2; b)1.0. (C) [GSH] = 4.6×10^{-5} M, [4-nitro-NBN] = 4.1×10^{-6} M, Tris/HCl 0.01 M, pH 7.5. Times (min): a) 0.45; b) 1.5; c) 2.2; d) After 10 min. (D) [GSH] = 4.9×10^{-5}, [4-nitro-NEHN] = 4.5×10^{-6}, Tris/HCl 0,01 M, pH 7.5. Time (min): a) 0.2; b) 1.0. [CTAC] = 9.8×10^{-4} M λ_{exc} (4-nitro-NBN) = 390 nm, λ_{exc} (4-nitro-NEHN) = 400 nm.

Additionally, the decrease of signal after thiol oxidation by hydrogen peroxide reinforces that the main fluorescence was due to the reaction of 4-nitro-NBN with thiols.

Since Cys residues at the extracellular surface of the cells are largely oxidized [31], the fluorescence is mostly due to the reaction of the probe with intracellular thiols. In addition, cells experiments were carried out in the absence of CTAC to avoid membrane disruption. The positive strong fluorescence indicates that 4-nitro-NBN can easily penetrate cell membranes and could be an effective thiol imaging probe in living cells. The 4-nitro-NEHN probe showed cytotoxicity, probably because of its long hydrophobic chain interaction with biological membrane (data not shown). Substituted naphtalimides have been used previously to quantify SH containing amino acids, peptides, proteins and detect SH groups in cells [32, 33, 34]. Song and collaborators used 4-nitro-1,8-naphthalimide derivatives to distinguish reaction with GSH and cysteine, however, due to the low water solubility of the probe, it was incubated with cells in 4:1 DMF:PBS and cell membrane integrity could be compromised [32].

These results indicate that 4-nitro-naphthalimides are good reagents for SH determination *in vitro* and *in vivo*. As opposed to the DTNB method, the SH group quantification needs the standard curve be done with a pure sample of the enzyme or thiol because the wavelengths of maximum excitation and fluorescence emission depend on the structure of the thiol,

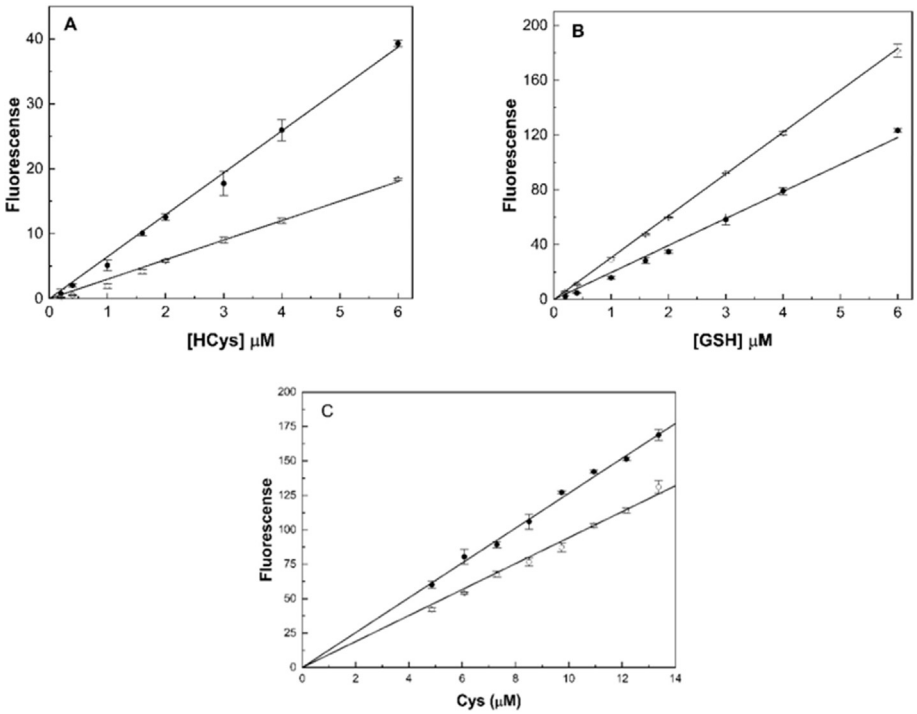

Figure 12. Fluorescence standard curves of the reaction's products of 4-nitro-NEHN and 4-nitro-NBN with HCys and GSH at different pHs. A) (●) [4-nitro-NBN] = 2.7×10^{-5} M, $R^2 = 0.998$ and slope = 6.4; (◯) [4-nitro-NEHN] = 2.7×10^{-5} M, MES (0.01 M), pH 6.5. $R^2 = 0.990$ and slope = 3.0. B) (●) [4-nitro-NBN] = 3.6×10^{-5} M, $R^2 = 0.988$ and slope = 16.7; (◯) [4-nitro-NEHN] = 2.7×10^{-5} M, Tris/HCl, 0.01 M, pH 7.0, $R^2 = 0.999$ and slope = 30.5. All experiments contained [CTAC] = 1.4×10^{-3} M. Fluorescence was read after 10 min. For 4-nitro-NBN, λ_{exc} = 390 nm, λ_{em} = 463 nm and for 4-nitro-NEHN, λ_{exc} = 400 nm, λ_{em} = 487 nm. C) Standard curves of Cys with 4-Nitro-NBN, $R^2 = 0.999$ and slope = 12.6 (●) and 4-nitro-NEHN (◯) in Tris/HCl 0.01M pH 8.0, $R^2 = 0.998$ and slope 9.4. The concentrations of 4-nitro-NEHN and 4-Nitro-NBN were 6.0×10^{-5} M and [CTAC] 1.5×10^{-3} M λ_{exc} = 390 nm; λ_{em} = 487 nm (Incubation time 1 h). Points are triplicate averages.

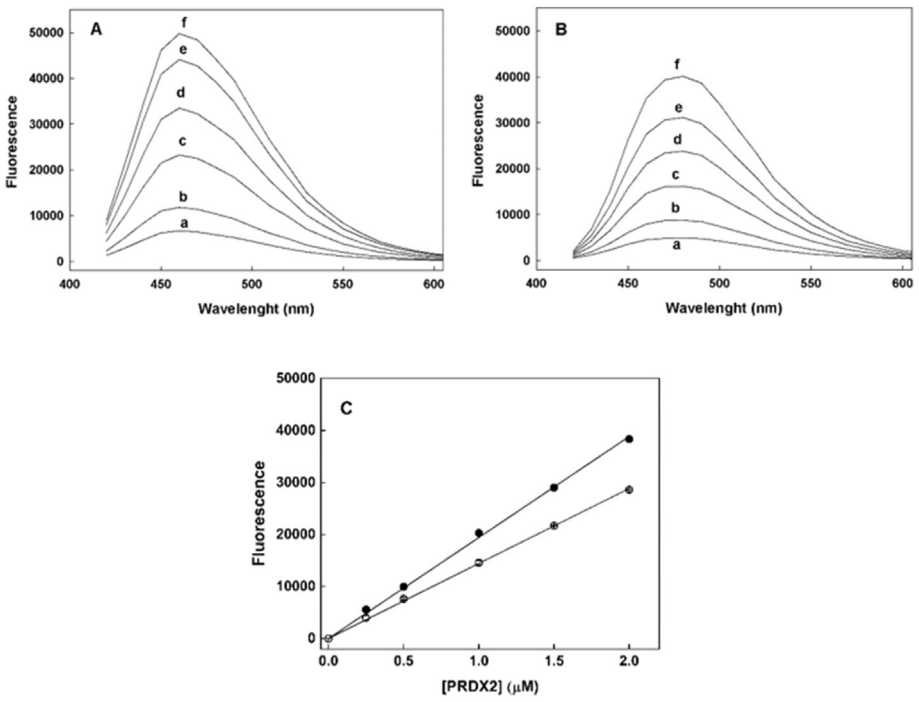

Figure 13. Fluorescence spectra of the products of the reaction of PRDX2 with 4-nitro-NEHN (A) and 4-nitro-NBN (B) at the end of the reaction (5 min) at different concentrations of PRDX2, [PRDX2] in Tris/HCl 0.01M, pH 7.5 buffer, 5 mM CTAC. The [PRX2] used were: a) 0.25; b) 0.5; c) 1.0; d) 1.5; e) 2.0 and f) 2.5 μM). (C) Standard curve of the fluorescence of the products of PRDX2 and nitro-naphthalimides, at the end of the reactions, vs [PRDX2]: (●) [4-nitro-NBN (R^2 = 0.995, slope = 20561 and (◯) 4-nitro-NEHN (R^2 = 0.999 and slope = 14408). The concentration of 4-nitro-NEHN and 4-nitro-NBN were 250 μM and the total volume was 0.4 mL. The λ_{exc} was 390 nm and λ_{em} was 470 nm. Points are averages of duplicates.

mainly if the thiol is in a protein. This does not happen to the DTNB method where the product, TNB, is the same, independently of the structure of the compounds containing SH groups. Also, a very interesting result was that the reaction occurred in the interior of the cells and the products of 4-nitro-naphthalimides with RSH were stable, differently from TNB which, in the presence of hydrogen peroxide or hypochlorous acid, is oxidized to the disulfide DTNB.

Interferences: care must be taken when doing the standard curves and samples for thiol determinations. For example, the presence of SDS, as well as phosphate buffers, interferes in the SH titration because CTAC will precipitate with both. High salt concentrations also must be avoided because the dissociation of the thiol groups with CTAC decreases with high salt concentrations and decreases the catalytic effect of CTAC. But these problems can be avoided diluting the protein samples in the buffer without these interferents.

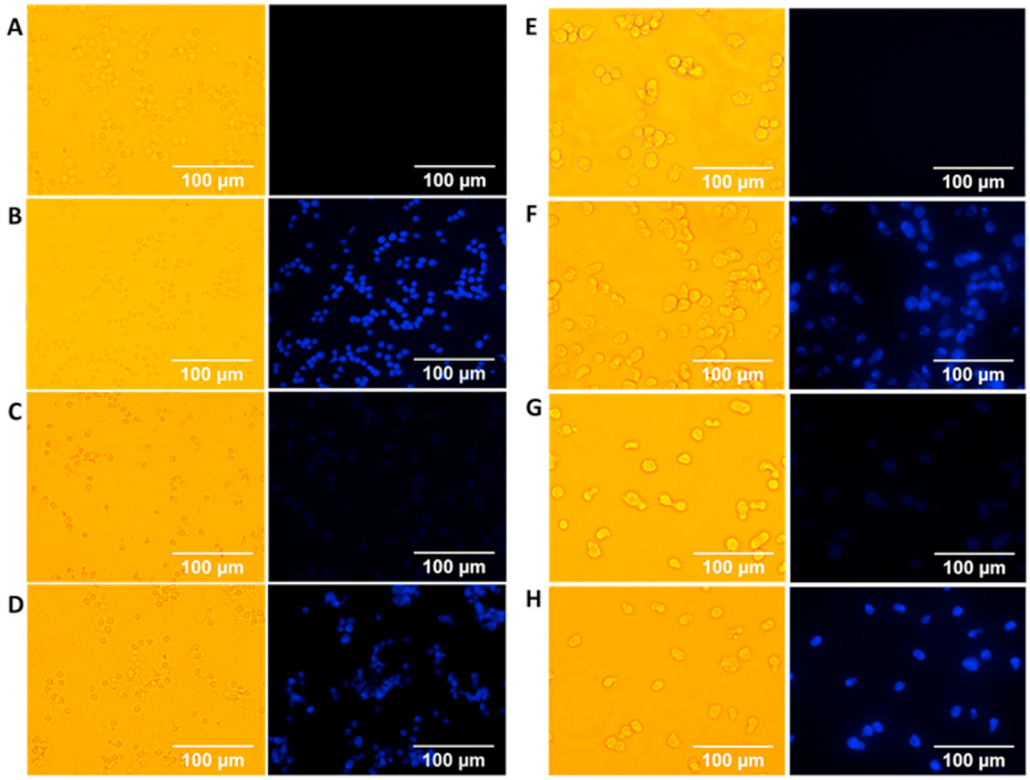

Figure 14. Fluorescence microscopy images of dHL-60 (left A-D) and dTHP-1 (right E-H). The cells (5×10^6 for dHL-60 or 2×10^6 for dTHP-1) were incubated at 37 °C in PBS/glucose. A and E controls without probe; B and F 100 μM 4-NBN for 30 min; C and G pre-incubated with 5 mM hydrogen peroxide for 15 min followed by 100 μM 4-NBN for 30 min and; D and H pre-incubated with 100 μM 4-NBN for 30 min followed by 5 mM hydrogen peroxide for 15 min. The images groups were captured in Nikon Eclipse TE300 (40 x objective lens) in phase contrast and fluorescence microscopy (excitation at UV light and emission detection with a blue filter).

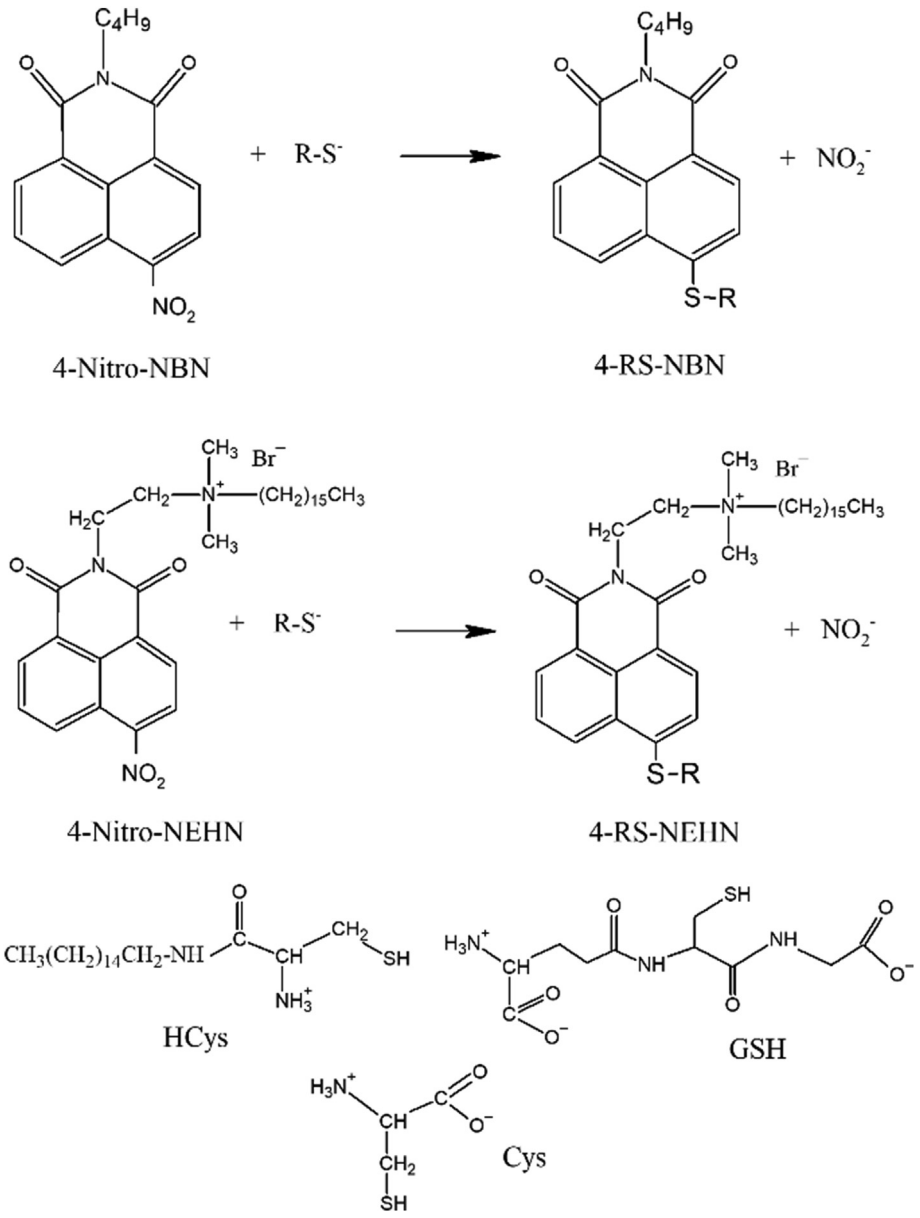

Scheme 1. Reactions between the thiols GSH, Cys and HCys with 4-Nitro-Alkyl-Naphthalimides (4-Nitro-NBN and 4-Nitro-NEHN) forming the thioethers 4-RS-NBN and 4-RS-NEHN.

Redox switches have an important role in cell signaling being involved in proliferation, differentiation, and death. In this sense, biological thiols such as glutathione and protein thiols (sulfhydryl groups) are important for maintaining redox homeostasis and participating in redox signaling [35]. So, it is of scientific and technological interest to detect thiol modifications. As sulfhydryl groups are nucleophiles, when dissociated, it is possible to chemically label protein thiols with specific agents and detect these modifications. 4-Nitro-NBN penetrated living cells and reacted with thiol groups. The pre-treatment of cells with hydrogen peroxide oxidized part of free thiol groups and prevented their reaction with the probe. The addition of hydrogen peroxide to the cells after the reaction of the probe with the thiols did not alter the fluorescence. These results support the idea that this probe can be used to detect the thiol status of the cell (reduced or oxidized). If cells are in oxidative stress, it is expected that thiols are oxidized and unable to react with the probe, otherwise if redox homeostasis is maintained, thiols are free to react with the probe and become fluorescent. In fact, it was proposed that other probes can react with thiols exhibiting fluorescence [13, 36, 37], showing that this is a promising technique.

4. Conclusions

The aromatic nucleophilic substitution reactions of the nitro group of 4-nitro-NEHN and 4-nitro-NBN by cysteine derivatives are strongly accelerated in micelle of CTAC. The reactions can occur at low pH and the acceleration factors can be of the order of 10^7 as compared with the reactions in aqueous phase.

4-nitro-NBN and 4-nitro-EHN, reacts with thiols in the presence of CTAC micelles and the products are not affected by oxidants like H_2O_2. Therefore, these nitro-naphthalimides are adequate reagents to quantify compounds containing SH groups.

The limit of detection of SH groups was as low as 5×10^{-7} M, ten times less than the limit for DTNB detection, at pHs between 6.5 and 7.5 which decreases the oxidation of the thiols.

The nitro-naphthalimides can also label SH groups in living cells and the fluorescence is not abolished by the presence of oxidants.

As the substitution reaction generates stable and fluorescent products, this reaction can be used as a convenient method for labeling proteins and peptides containing –SH groups.

Declarations

Author contribution statement

Iolanda Midea Cuccovia: Conceived and designed the experiments; Performed the experiments; Analyzed and interpreted the data; Contributed reagents, materials, analysis tools or data; Wrote the paper.

Vanessa S Martins, João S Bonilha, Larissa M Gonçalves, Laura Mortara, Larissa AC Carvalho, Bhaskar R Manda, Carolina D Lacerda: Performed the experiments.

Eduardo R Triboni: Conceived and designed the experiments; Performed the experiments; Contributed reagents, materials, analysis tools or data.

Flavia C Meotti: Conceived and designed the experiments; Analyzed and interpreted the data; Contributed reagents, materials, analysis tools or data; Wrote the paper.

Mario J Politi: Conceived and designed the experiments.

Hernan Chaimovich: Analyzed and interpreted the data; Wrote the paper.

Funding statement

Larissa AC Carvalho was supported by Fundação de Amparo à Pesquisa do Estado de São Paulo (2013/02195-3). Larissa M Gonçalves was supported by Fundação de Amparo à Pesquisa do Estado de São Paulo (18/19838-8). Bhaskar R Manda was supported by Fundação de Amparo à Pesquisa do Estado de São Paulo (2016/00709-8). Eduardo R Triboni was supported by Fundação de Amparo à Pesquisa do Estado de São Paulo (2018/15214-0). Iolanda Midea Cuccovia was supported by Fundação de Amparo à Pesquisa do Estado de São Paulo (2013/0866-5; 2015/10411-3). Flavia C Meotti was supported by Fundação de Amparo à Pesquisa do Estado de São Paulo (11/18106-4; 18/14898-2). Hernan Chaimovich was supported by Conselho Nacional de Desenvolvimento Científico e Tecnológico (301907/2019-6). Iolanda Midea Cuccovia was supported by Conselho Nacional de Desenvolvimento Científico e Tecnológico (302490/2017-5).

Competing interest statement

The authors declare no conflict of interest.

Additional. information

No additional information is available for this paper.

Acknowledgements

The authors thank Dr. Fernanda Manso Prado and Dr. Paolo Di Mascio (from Instituto de Química, USP) for the mass spectrometry data. We deeply thank Dr. Dalva Lúcia Araújo de Farias from the Laboratory of Molecular Spectroscopy, Dr. Alcindo Aparecido dos Santos, Felipe Wodtke and Marcos Vinicio Lopes Rodrigues Archilha all from IQUSP for helping us with new experiments to answer the reviews in a such uneasy time, as the personal and institutional activities are compromised by the pandemic.

References

[1] G. Roos, N. Foloppe, J. Messens, Understanding the pKa of redox cysteines: the key role of hydrogen bonding, Antioxidants Redox Signal. 18 (2013) 94–127.

[2] C. Jacob, G.I. Giles, N.M. Giles, H. Sies, Sulfur and selenium: the role of oxidation state in protein structure and function, Angew. Chem. Int. Ed. 42 (2003) 4742–4758.

[3] R.E. Benesch, R. Benesch, The acid strength of the -SH group in cysteine and related compounds, J. Am. Chem. Soc. 77 (1955) 5877–5881.

[4] J.P. Danehy, C.J. Noel, The relative nucleophilic character of several mercaptans toward ethylene oxide, J. Am. Chem. Soc. 82 (1960) 2511–2515.

[5] G. Jung, E. Breitmaier, W. Voelter, Dissoziationsgleichgewichte von Glutathion, Eur. J. Biochem. 24 (1972) 438–445.

[6] M.S. Ning, S.E. Price, J. Ta, K.M. Davies, Nucleophilic reactivity of thiolate, hydroxide, and phenolate ions toward a model O2-arylated diazeniumdiolate prodrug in aqueous and cationic surfactant media, J. Phys. Org. Chem. 23 (2010) 220–226.

[7] W.P. Jencks, Catalysis in Chemistry and Enzymology, Dover Publications, 1987.

[8] J. Reijenga, A. van Hoof, A. van Loon, B. Teunissen, Development of methods for the determination of pKa values, Anal. Chem. Insights 8 (2013) 53–71.

[9] S.D. Copley, W.R.P. Novak, P.C. Babbitt, Divergence of function in the thioredoxin fold suprafamily: evidence for evolution of peroxiredoxins from a thioredoxin-like ancestor, Biochemistry 43 (2004) 13981–13995.

[10] L.E.S. Netto, M.A. de Oliveira, G. Monteiro, A.P.D. Demasi, J.R.R. Cussiol, K.F. Discola, M. Demasi, G.M. Silva, S.V. Alves, V.G. Faria, B.B. Horta, Reactive cysteine in proteins: protein folding, antioxidant defense, redox signaling and more, Comp. Biochem. Physiol. C Toxicol. Pharmacol. 146 (2007) 180–193.

[11] D. Barford, B.G. Neel, Revealing mechanisms for SH2 domain mediated regulation of the protein tyrosine phosphatase SHP-2, Structure 6 (1998) 249–254.

[12] L. Ma, J. Qian, H. Tian, M. Lan, W. Zhang, A colorimetric and fluorescent dual probe for specific detection of cysteine based on intramolecular nucleophilic aromatic substitution, Analyst 137 (2012) 5046–5050.

[13] P. Zhou, J. Yao, G. Hu, J. Fang, Naphthalimide scaffold provides versatile platform for selective thiol sensing and protein labeling, ACS Chem. Biol. 11 (2016) 1098–1105.

[14] E.R. Triboni, J.C. Artur, P.B. Filho, L.M. Cuccovia, M.J. Politi, Aromatic nitro substitution reaction between 4-nitro-N-n-butyl-1,8- naphthalimide and n-heptanethiol in water-methanol binary mixtures, J. Phys. Org. Chem. 22 (2009) 703–708.

[15] E.R. Triboni, M.J. Politi, I.M. Cuccovia, H. Chaimovich, P. Berci Filho, Rate-limiting step and micellar catalysis of the non-classical nitro group nucleophilic substitution by thiols in 4-nitro-N-n-butyl-1,8-naphthalimide, J. Phys. Org. Chem. 16 (2003) 311–317.

[16] F.H. Quina, H. Chaimovich, Ion exchange in micellar solutions 1 conceptual framework for ion exchange in micellar solutions, J. Phys. Chem. 83 (1979) 1844–1850.

[17] G.L. Ellman, Tissue sulfhydryl groups, Arch. Biochem. Biophys. 82 (1959) 70–77.

[18] L.M. Landino, C.B. Mall, J.J. Nicklay, S.K. Dutcher, K.L. Moynihan, Oxidation of 5-thio-2-nitrobenzoic acid, by the biologically relevant oxidants peroxynitrite anion, hydrogen peroxide and hypochlorous acid, Nitric Oxide - Biol. Chem. 18 (2008) 11–18.

[19] C.K. Riener, G. Kada, H.J. Gruber, Quick measurement of protein sulfhydryls with Ellman's reagent and with 4,4′-dithiodipyridine, Anal. Bioanal. Chem. 373 (2002) 266–276.

[20] H. Chaimovich, J.B.S. Bonilha, D. Zanette, I.M. Cuccovia, Analysis of the effects of micelles and vesicles on the reactivity of nucleophiles derived from dissociation of weak acids, in: B. Lindman, K.L. Mittal (Eds.), Surfactants Solut., 1983.

[21] E. Castaldelli, E.R. Triboni, G.J.F. Demets, Self-assembled naphthalenediimide derivative films for light-assisted electrochemical reduction of oxygen, Chem. Commun. 47 (2011) 5581–5583.

[22] S.S. Rhee, D.H. Burke, Tris(2-carboxyethyl)phosphine stabilization of RNA: comparison with dithiothreitol for use with nucleic acid and thiophosphoryl chemistry, Anal. Biochem. 325 (2004) 137–143.

[23] P.W. Riddles, R.L. Blakeley, B. Zerner, Reassessment of Ellman's reagent, Methods Enzymol. 91 (1983) 49–60.

[24] O. Schales, S.S. Schales, A simple and accurate method for the determination of chloride in biological fluids, Anal. Chem. 140 (1941) 879–884.

[25] S.G. Tajc, S.G. Tajc, B.S. Tolbert, B.S. Tolbert, R. Basavappa, R. Basavappa, B.L. Miller, B.L. Miller, Direct determination of thiol pK, J. Am. Chem. Soc. 14642 (2004) 10508–10509.

[26] J.D. Hopton, C.J. Swan, D.L. Trimm, Liquid-phase oxidation of thiols to disulfides, in: F.R. Mayo (Ed.), Oxid. Org. Compd., Advances in Chemistry, American Chemical Society, Washington, DC, 1968, pp. 216–224.

[27] H. Chaimovich, J.B.S. Bonilha, M.J. Politi, F.H. Quina, Ion exchange in micellar solutions 2 binding of hydroxide ion to positive micelles, J. Phys. Chem. 83 (1979) 1851–1854.

[28] Z.H. Chae, S.J. Chung, S.G. Rhee, Thioredoxin-dependent peroxide reductase from yeast, J. Biol. Chem. 269 (1994) 27670–27678.

[29] R. Kumari, D. Sunil, R.S. Ningthoujam, Naphthalimides in fluorescent imaging of tumor hypoxia – an up-to-date review, Bioorg. Chem. 88 (2019) 102979.

[30] P. Wardman, E.D. Clarke, Oxygen inhibition of nitroreductase: electron transfer from nitro radical-anions to oxygen, Biochem. Biophys. Res. Commun. 69 (1976) 942–949.

[31] M.F. Mineiro, E.S. de Patricio, Á.S. Peixoto, T.L.S. Araujo, R.P. da Silva, A.I.S. Moretti, F.S. Lima, F.R.M. Laurindo, F.C. Meotti, Urate hydroperoxide oxidizes endothelial cell surface protein disulfide isomerase-A1 and impairs adherence, Biochim. Biophys. Acta Gen. Subj. 1864 (2020) 129481.

[32] L. Song, J. Lun, L. Ti, W. Lu, N. Jia, W. Zhang, J. Qian, Multi-channel colorimetric and fluorescent probes for differentiating between cysteine and glutathione/homocysteine, Org. Biomol. Chem. 12 (2014) 8422–8427.

[33] L. Zhou, L. Xie, C. Liu, Y. Xiao, New trends of molecular probes based on the fluorophore 4-amino-1,8-naphthalimide, Chin. Chem. Lett. 30 (2019) 1799–1808.
[34] Y.-F. Kang, Li-Y. Niu, Q.-Z. Yang, Fluorescent probes for detection of biothiols based on "aromatic nucleophilic substitution-rearrangement" mechanism, Chin. Chem. Lett. 30 (2019) 1791–1798.
[35] K.M. Holmström, T. Finkel, Cellular mechanisms and physiological consequences of redox-dependent signalling, Nat. Rev. Mol. Cell Biol. 15 (2014) 411–421.
[36] X. Chen, Y. Zhou, X. Peng, J. Yoon, Fluorescent and colorimetric probes for detection of thiols, Chem. Soc. Rev. 39 (2010) 2120–2135.
[37] J. Shi, Y. Wang, X. Tang, W. Liiu, H. Jiang, W. Dou, W. Liu, A colorimetric and fluorescent probe for thiols based on 1, 8-naphthalimide and its application for bioimaging, Dyes Pigments 100 (2014) 255–260.